5th International Conference on Mathematical Modeling in Physical Sciences (IC-MSquare 2016) IOP Publishing
Journal of Physics: Conference Series **738** (2016) 012022 doi:10.1088/1742-6596/738/1/012022

Convex and concave successions of power-law decays in small-angle scattering

E M Anitas[1,2]

[1]Joint Institute for Nuclear Research, Dubna 141980, Moscow region, Russia
[2]Horia Hulubei National Institute of Physics and Nuclear Engineering, RO-077125 Bucharest, Romania

E-mail: anitas<at>theor.jinr.ru

Abstract. The small-angle scattering (SAS) structure factor from a new model of a 3D deterministic fractal in which the relative positions and the number of structural units vary with fractal iteration number is calculated. It is shown that, depending on the relative positions of scattering units inside the fractal, we can obtain various types of power-law successions, such as: convex/concave - when the absolute value of the scattering exponent of the first power-law decay is higher/smaller than that of the subsequent power-law decay, or any combination of them (i.e. convex-concave or concave-convex). The obtained results can explain experimental SAS (neutron or X-rays) data which are characterized by a succession of power-law decays of arbitrary length.

1. Introduction

Small-angle scattering is a well established technique [1, 2] for determination of structural properties of complex nano and micro systems such as: aggregation processes in polymeric solutions [3], morphology of crystalline amorphous block copolymers in solution [4], microstructure of elastomeric/composite membranes [5, 6], and is especially suited for those structures which are characterized by either exact or statistical self-similarity (deterministic and random fractals; [7–9]). Its main advantage is the possibility to distinguish between mass and surface fractals [10–14] through the value of the scattering exponent τ from the power-law dependence $I(q) \propto q^{-\tau}$, where $\tau = D_{\rm m}$ for mass fractals ($0 < D_{\rm m} < 3$), and $\tau = 6 - D_{\rm s}$ for surface fractals ($2 < D_{\rm s} < 3$). Here, $D_{\rm m}$ and $D_{\rm s}$ denote the mass, and respectively the surface fractal dimension, and q is the scattering vector magnitude.

For random fractals, besides the fractal dimension, one may obtain the overall size of the fractal from the Guinier region, and the size of the smallest structural 'subunit' composing the fractal, from the end of the fractal region. For deterministic fractals with a single scale it has been shown that additional structural information can be obtained from experimental SAS data, such as: the iteration number, the fractal scaling factor, or the total number of structural subunits composing the fractal [15, 16].

However, some experimental SAS data [17–21] show a succession of power-law decays with arbitrarily scattering exponents, and recently few theoretical models have been proposed both, for 'convex' / 'concave' data (where the absolute value of the scattering exponent of the first power-law regime is higher/smaller than that of the next power-law regime) [22, 23]. While for 'convex' data the model assumes a three-phase structure in which homogeneous structures with scattering length densities ρ_1 and ρ_2 are immersed in a homogeneous medium with density ρ_0, for the 'concave' data the basic assumption is a two-phase system in which the homogeneous structures of scattering length density ρ_1 are fractals whose scaling factor varies with iteration number.

In this work we develop a new theoretical model based on deterministic mass fractals with a single scale, and we show that the behavior given by a succession of 'convex' / 'concave' SAS data, and more generally, by any combination of them, can be explained also by a two-phase system in which the relative positions and the number of structural subunits vary with fractal iteration number.

2. Models

In building our models, we consider a top-down approach in which a cube of edge l_0 with a ball of radius $r_0 = l_0/2$ in its center (initiator) is repeatedly divided in smaller pieces according to some prescribed rules (see below). We choose a Cartesian system of coordinates whose center coincide with the center of the initiator. The iteration rule consists in replacing the cube of edge l_0 with a given number $k_1 > 1$ of smaller cubes of edge length $l_1 = l_0/3$ (first iteration). Then, at m-th iteration the edge of the cube is $l_m = l_0/3^m$ and the radii of concentric balls are $r_m \equiv l_m/2 = r_0/3^m$. Here, we choose three different fractals (Fig. 1) with a significant difference in their fractal dimensions $D_{\rm m}$ so that also the differences in the slopes of scattering structure factor and the succession of 'convex'/'concave' power-law regimes to be easily recognized.

The so-obtained fractals consist of subunits with scattering length density ρ_u immersed in a solid matrix of scattering length density ρ_m. Thus, the scattering contrast will be given by $\Delta\rho = \rho_u - \rho_p$ and the scattering intensity becomes [1]:

$$I(q) = n\,|\Delta\rho|^2\,V^2\langle|F(\boldsymbol{q})|^2\rangle, \tag{1}$$

where n is the concentration of fractals, V is their volume, the angle brackets $\langle\cdots\rangle$ is the averaging over all possible orientations, and $F(\boldsymbol{q}) \equiv (1/V)\int_V e^{-i\boldsymbol{q}\cdot\boldsymbol{r}}\mathrm{d}\boldsymbol{r}$ is the normalized form factor.

We choose configurations in such a way that the scattering units are positioned symmetric with respect to the origin, and their number at m-th iteration is given by

$$k_m = \begin{cases} 8^m, & for\ fractal\ I, \\ 14^m, & for\ fractal\ II, \\ 20^m, & for\ fractal\ III. \end{cases} \tag{2}$$

Note that *fractal-I* is the well known triadic Cantor set, and *fractal-III* is the Menger sponge. Thus, the fractal dimensions are obtained in the limit of infinite number of iterations, and is given by [15]

$$D_{\rm m} = \lim_{m\to\infty}\frac{\log k_m}{\log(1/3)} = \begin{cases} 1.89, & for\ fractal\ I, \\ 2.40, & for\ fractal\ II \\ 2.71, & for\ fractal\ III. \end{cases} \tag{3}$$

According to the number of subunits given by Eq. (2), the corresponding generative function describing the relative positions of scattering subunits inside each fractal, can be written as:

$$G_m(\boldsymbol{q}) = \begin{cases} \Lambda_m(\boldsymbol{q}), & for\ fractal\ I, \\ \dfrac{1}{14}\left(8\Lambda_m(\boldsymbol{q}) + 2\Gamma_m(\boldsymbol{q})\right), & for\ fractal\ II \\ \dfrac{1}{20}\left(8\Lambda_m(\boldsymbol{q}) + 4\Gamma_m(\boldsymbol{q})\right), & for\ fractal\ III, \end{cases} \tag{4}$$

where $\Lambda_m(\boldsymbol{q}) \equiv \cos(l_m q_x)\cos(l_m q_y)\cos(l_m q_z)$, $C_m(\boldsymbol{q}) \equiv \cos(l_m q_x) + \cos(l_m q_y) + \cos(l_m q_z)$, and $\Gamma_m(\boldsymbol{q}) \equiv \cos(l_m q_x)\cos(l_m q_y) + \cos(l_m q_x)\cos(l_m q_z) + \cos(l_m q_y)\cos(l_m q_z)$ (Fig. 1).

Each of the individual fractal in Fig. 1 gives rise to a single power-law decay (with $\tau = D_{\rm m}$) in the scattering intensity. Thus, in order to observe *a succession* of power-law decays with different

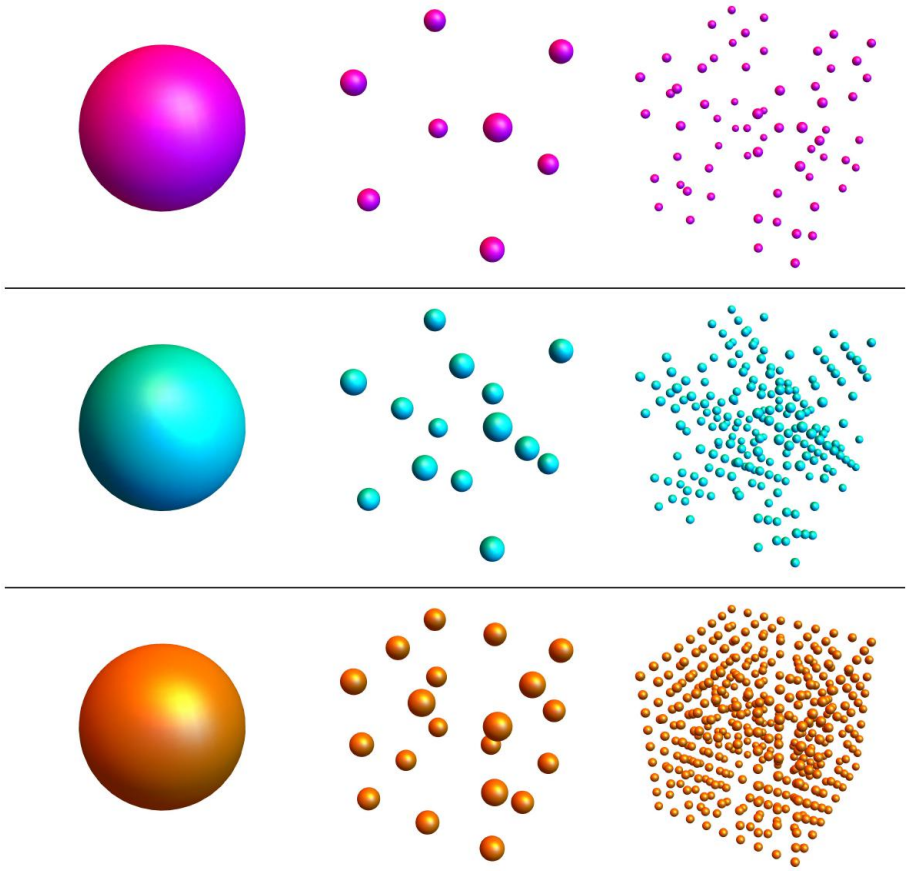

Figure 1. The initiator and first two iterations for models with $k_m = 4^m$ (upper fractal), $k_m = 8^m$ (middle fractal) and $k_m = 12^m$ (lower fractal), for arbitrarily iteration m.

exponents, we proceed as follows: for the first p iterations we consider the structure of a single fractal (from those defined in Eq. (2)), for the next q iterations we consider the structure of another fractal (also from those defined in Eq. (2)), and finally, for the next r iterations we consider the structure of the remaining fractal. Thus, depending on the particular fractal chosen for each p, q or r iterations, we shall expect any of the following type of successions of power-law decays: $q^{-1.89} \to q^{-2.40} \to q^{-2.71}$ ('concave' succession), $q^{-2.71} \to q^{-2.40} \to q^{-1.89}$ ('convex' succession), $q^{-2.40} \to q^{-2.71} \to q^{-1.89}$, or $q^{-2.40} \to q^{-1.89} \to q^{-2.71}$. For simplicity, in the following we choose $p = q = r = 2$ for each type of succession. However, the length of each individual fractal region can be varied by changing any of the values of p, q or r.

3. Scattering structure factor

In order to calculate the monodisperse scattering structure factor, we neglect the shape of fractal subunits, and thus, using Eq. (2) together with Eq. (4) we can write [15, 16]:

$$S_m^{\text{mono}}(q) = k_m \langle \prod_{i=1}^{m} |G_i(\boldsymbol{q})|^2 \rangle. \tag{5}$$

Then, the polydispersity involves a system of various sizes l, and the distribution function $D_N(l)$ is defined in such a way that $D_N(l)\mathrm{d}l$ represents the probability of finding a fractal with sizes between

$(l, \mathrm{d}l)$. Therefore, the polydisperse structure factor given by Eq. (5) becomes:

$$S_m^{\mathrm{poly}}(q) = k_m \int_0^\infty \langle \prod_{i=1}^{m} |G_i(\boldsymbol{q})|^2 \rangle D_N(l) \mathrm{d}l. \tag{6}$$

In the following, a log-normal distribution of mean length $\mu_0 \equiv \langle l \rangle_D$ and relative variance $\sigma_r = (\langle l^2 \rangle_D - l_0^2)^{1/2}/l_0$ is considered.

4. Results and discussions

In order to obtain all the possible combinations of power-law successions we consider the following types of fractals: $Type\ I$ - a fractal consisting of $fractal\ I$ for first two iterations, followed by $fractal\ II$ for 3-rd and 4-th iteration, and $fractal\ III$ for 5-th and 6-th iterations. In this way, the monodisperse structure factor is characterized by the following sequence of generalized power-law regimes [15] $q^{-1.89} \rightarrow q^{-2.40} \rightarrow q^{-2.71}$ (Fig. 2a - black curve). The succession of simple power-law regimes, as obtained in most of the experimental data, are recovered by taking into account the polydispersity, as discussed in section (3)/ The numerical results are presented in Fig. 2a - red curve, which clearly show the succession of simple regimes with decreasing absolute values of the power-law exponent, i.e. a 'concave' scattering curve.

The other possible combinations of power-law successions are obtained similar as for $fractal\ I$. For example, the $fractal\ II$ structure is built from the fractal consisting of $fractal\ II$ for first two iterations, followed by $fractal\ III$ at 3-rd and 4-th iterations, and then $fractal\ I$ at 5-th and 6-th iterations. The corresponding mono and polydisperse structure factor are shown in Fig. 2b (black, and respectively red curves), which clearly reveals a combination of 'concave' scattering corresponding to transition $q^{-2.40} \rightarrow q^{-2.71}$ followed by a 'convex' scattering corresponding to transition from $q^{-2.71} \rightarrow q^{-1.89}$. The results corresponding to SAS from $TypeIII$ and $TypeIV$ are shown in Fig. 2c and d, which illustrates the other possible transitions: $q^{-2.40} \rightarrow q^{-1.89} \rightarrow q^{-2.71}$, and respectively $q^{-2.71} \rightarrow q^{-2.40} \rightarrow q^{-1.89}$.

For all the considered $Types$, one can observe that beyond the last generalized/simple power law-decay we have $q > 1/(\beta_{\mathrm{s}}^m l_0)$, and thus the structure factors shown in Fig. 2a-d tend to one. This implies that the asymptotic values are $1/k_m$ (see Eq. 2), which is in agreement with the numerical results (horizontal lines in Fig. 2a-d).

5. Conclusion

We have built a new theoretical model based on fractal structures which can explain experimental small-angle scattering curves characterized by a succession of power-law decays. Its main feature consists in changing the construction rule of the fractal after a finite number of iterations (here, at every second iteration), which give rise to a succession of power-law decays with different scattering exponents. We confirmed this by performing analytical calculations of mono and polydisperse structure factor. In addition, the obtained structure factor allows us to obtain the number of subunits in each fractal, from the asymptotic values at high q.

The proposed model is based on deterministic mass fractals and can be applied to 'convex'/'concave' data or any combination of them.

References

[1] Feigin L A and Svergun D I 1987 *Structure Analysis by Small-Angle X-Ray and Neutron Scattering* (NY: Plenum press)
[2] Glatter O and Kratky O 1982 *Small-angle X-ray Scattering* (London: Academic Press)
[3] Dumoulin M, Hamd W, Thune E, Rochas C and Guinebretiere R 2016 *J. Appl. Cryst.* **49** 1–9
[4] Radulescu A, Goerigk G and Richter D 2015 *J. Appl. Cryst.* **48** 1860–1869
[5] Anitas E M, Bica I, Erhan R V, Bunoiu M and Kuklin A I 2015 *Rom. Journ. Phys.* **60** 653–657
[6] Bica I, Anitas E M, Averis L M E and Bunoiu M 2015 *J. Ind. Eng. Chem.* **21** 1323–1327

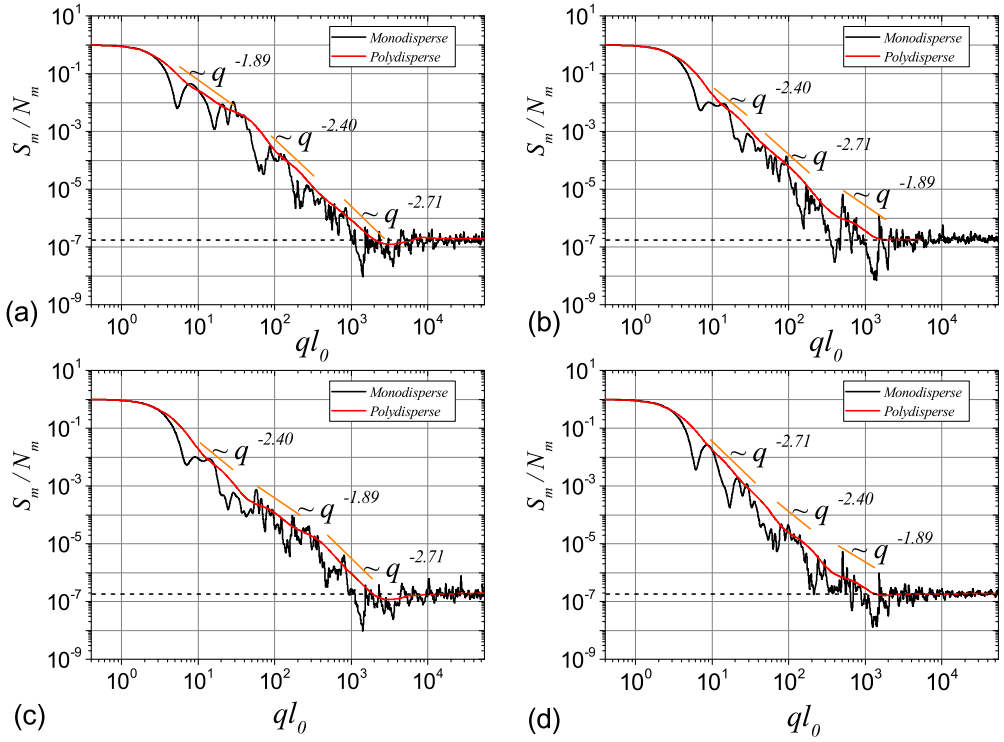

Figure 2. The fractal structure factor for first six iterations. a) *Type I*; b) *Type II*; c) *Type III*; and d) *Type IV* structures (see description in text for each *Type*).

[7] Gouyet J F 1996 *Physics and Fractal Structures* (Springer)
[8] Turcotte D L 1997 *Fractals and Chaos in Geology and Geophysics* (Cambridge University Press)
[9] Hamburger-Lidar D A 1996 *Phys. Rev. E* **54** 354
[10] Bale H D and Schmidt P W 1984 *Phys. Rev. Lett.* **53** 596
[11] Martin J E and Hurd A J 1987 *J. of Appl. Cryst.* **20** 61–78
[12] Teixeira J 1988 *J. Appl. Cryst.* **21** 781
[13] Schmidt P W 1991 *J. of Appl. Cryst.* **24** 414–435
[14] Beaucage G 1995 *J. Appl. Cryst.* **28** 717
[15] Cherny A Y, Anitas E M, Kuklin A I and Osipov V A 2011 *Phys. Rev. E* **84** 036203–1–036203–11
[16] Cherny A Y, Anitas E M, Osipov V A and Kuklin A I 2015 *Rom. Journ. Phys* **60** 658–663
[17] Balasoiu M, Craus M L, Kuklin A I, Plestil J, Haramus V, Islamov A H, Erhan R V *et al.* 2008 *Journal of Optoelectronics and Advanced Materials* **10** 2932–2935
[18] Zhao J, Shi D and Lian J 2009 *Carbon* **47** 2329
[19] Anitas E M, Balasoiu M, Bica I, Osipov V A and Kuklin A I 2009 *Optoelectronics and Advanced Materials - Rapid Communications* **3** 621–624
[20] Headen T F, Boek E S, Stellbrink J and M S U 2009 *Langmuir* **2** 422
[21] Golosova A A, Adelsberger J, Sepe A, Niedermeier M A, Lindner P, Funari S S, Jordan R *et al.* 2012 *J. Phys. Chem. C* **116** 15765
[22] Cherny A Y, Anitas E M, Osipov V A and Kuklin A I 2014 *J. Appl. Cryst.* **47** 198–206
[23] Anitas E M 2014 *Eur. Phys. J. B* **87** 139